



Rapid examination of the kinetic process of intramolecular lactamization of gabapentin using DSC–FTIR

Cheng-Hung Hsu, Shan-Yang Lin*

Lab. Pharm. Biopharm., Department of Biotechnology, Yuanpei University, Hsin Chu, Taiwan, ROC

ARTICLE INFO

Article history:

Received 23 October 2008

Received in revised form 6 December 2008

Accepted 8 December 2008

Available online 13 December 2008

Keywords:

Gabapentin

Gabapentin-lactam

Intramolecular cyclization

DSC

TG

DSC–FTIR

ABSTRACT

The thermal stability and thermodynamics of gabapentin (GBP) in the solid state were investigated by DSC and TG techniques, and FTIR microspectroscopy. The detailed intramolecular lactamization process of GBP to form gabapentin-lactam (GBP-L) was also determined by thermal FTIR microspectroscopy. GBP exhibited a DSC endothermic peak at 169 °C. The weight loss in TG curve of GBP suggested that the evaporation process of water liberated via intramolecular lactamization was simultaneously combined with the evaporation process of GBP-L having a DSC endothermic peak at 91 °C. A thermal FTIR microspectroscopy clearly evidenced the IR spectra at 3350 cm⁻¹ for water liberated and at 1701 cm⁻¹ for lactam structure formed due to the lactam formation of GBP. This study indicates that the activation energy for combined processes of intramolecular lactamization of GBP and evaporation of GBP-L was about 114.3 ± 23.3 kJ/mol, but for the evaporation of GBP-L alone was 76.2 ± 1.5 kJ/mol. A powerful simultaneous DSC–FTIR combined technique was easily used to quickly examine the detailed kinetic processes of intramolecular cyclization of GBP and evaporation of GBP-L in the solid state.

© 2008 Elsevier B.V. All rights reserved.

1. Introduction

Gabapentin (GBP) with a trade name of Neurontin® is extensively used for the treatment of convulsive-type cerebral disorders, such as epilepsy, hypokinesia and cranial trachoma [1]. GBP has also shown a pain-relieving property for management of the neuropathic pain of patient [2]. Moreover, the anti-anxiety activity of GBP in treating neurodegenerative diseases like Alzheimer's is also demonstrated [3]. Since GBP is structurally related to the neurotransmitter of γ -aminobutyric acid (GABA), thus it has been designed as a GABA-mimetic agent to freely cross the blood–brain barrier, resulting in higher level of GBP in the brain for treatment of partial seizures [4,5].

Although GBP is very soluble in water and well absorbed, it is susceptible to degradation into an impurity known as gabapentin-lactam (GBP-L) via intramolecular cyclization [6]. This GBP-L product has been found to cause a higher toxicity than GBP [7]. As impurity, the presence of lactam in GBP pharmaceutical products during the manufacturing process and/or storage condition should be limited or prevented, though GBP-L is currently under investigation for its pronounced neuroprotective activity and neurotrophic effect [8,9]. The chemical structures of GBP and GBP-L are compared in Fig. 1.

Recently, solid-state chemistry of drug is of growing importance in the pharmaceutical industry for developing the useful API (active pharmaceutical ingredient) of drug and stable dosage forms [10–12]. It has been reported that GBP exists as a zwitterion in the solid state and also exhibits different polymorphs [13–15]. Until now, however, only a few reports describing the solid-state thermal stability of GBP [14,16]. The thermodynamics and detailed kinetic process of lactamization of GBP in the solid state are unclear. The aim of this study was to investigate the solid-state physico-chemical properties and lactamization of GBP by using differential scanning calorimetry (DSC), thermogravimetric (TG) analysis and Fourier transform infrared (FTIR) microspectroscopy. Furthermore, a novel simultaneous DSC–FTIR combined technique was also used to elaboratively explore the process of lactamization of GBP. The kinetics and activation energies of GBP in the solid state during the processes of intramolecular lactamization and thermal stability of GBP-L were also determined by TG analysis.

2. Materials and methods

2.1. Materials

A pharmaceutical grade of gabapentin (GBP, Batch No. PN63415, Sun Pharma. Ind. Ltd., Gujarat, India) was kindly supplied by Orient Europharma Co. Ltd. (Taoyuan, Taiwan, ROC) and used without further purification. This commercial API of GBP used in this study was proven to be a polymorphic form II [15,17]. An analytical reagent

* Corresponding author. Tel.: +886 3 5381183x8157; fax: +886 3 6102328.
E-mail address: sylin@mail.ypu.edu.tw (S.-Y. Lin).

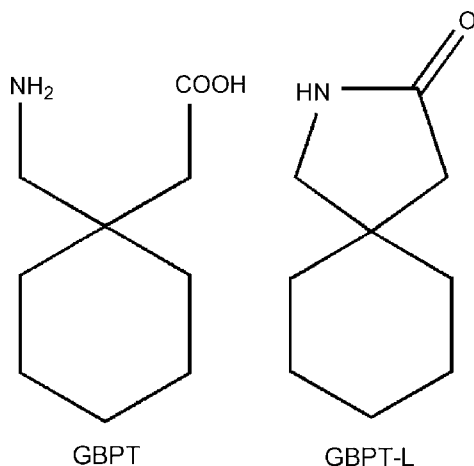


Fig. 1. The chemical structures of GBP and GBP-L.

grade of KBr cubic crystal (5 mm × 5 mm × 5 mm, Jasco Co., Tokyo, Japan) was cut into thin plate-like pieces for use.

2.2. Sample preparation

The GBP-L was prepared by directly heating the GBP sample to 176 °C in DSC system (DSC-910, TA Instruments Inc., New Castle, DE, USA), and then cooling to 25 °C. Different pretreated samples of GBP were respectively prepared by preheating GBP powder to different prescribed temperatures (147–197 °C) in this DSC system, and then slowly cooling to 25 °C by using a refrigerated cooling system. The evaporated GBP-L after DSC determination was also collected from the top place of DSC furnace.

2.3. Analytical identification

All the GBP and GBP-L samples were determined using Fourier transform infrared (FTIR) microspectroscopy (Micro FTIR 200, Jasco Co., Tokyo, Japan) with 2KBr method (sample was sealed within two KBr pellets) by transmission technique [18,19], and also measured by differential scanning calorimetry (DSC, TA Instruments Inc., New Castle, DE, USA) at a heating rate of 3 °C/min with an open pan system in a stream of N₂ gas from 30 to 260 °C. FTIR spectra were generated by co-addition of 256 interferograms collected at 4 cm⁻¹ resolution. Temperature and heat flow of DSC system were calibrated by standard indium sample. Thermogravimetric (TG) analysis (TGA-951, TA Instruments Inc., New Castle, DE, USA) was also carried out by using the different heating rates (2–15 °C/min) to measure the weight loss of GBP and GBP-L samples. All the thermal analyses were highly reproducible in terms of shape and thermal transition values for three runs.

2.4. Study of DSC–FTIR combined technique

Another trace of each GBP or GBP-L sample was directly pressed on one piece of KBr pellet (1KBr method) or sealed within two pieces of KBr pellets (2KBr method) by a hydraulic press under 200 kg/cm² for 15 s to form a disc [18,19]. Each disc was placed onto a micro hot stage (DSC microscopy assembly, FP 84, Mettler, Greifensee, Switzerland). The DSC microscopy assembly was then directly placed on the stage of a FTIR microscopic spectrometer with a mercury cadmium telluride (MCT) detector in the transmission method (DSC–FTIR combined technique). The system was operated in transmission mode. The temperature of the DSC microscopy assembly was monitored with a central processor (FP 80HT, Mettler, Switzerland), and its heating rate was maintained at 3 °C/min

under 25–28 °C/65–75% RH condition. Each sample disc was equilibrated to the starting temperature (30 °C) and then heated to 200 °C. The thermal-responsive IR spectra were simultaneously recorded during heating [18,19].

3. Results and discussion

3.1. Thermal analysis of GBP and GBP-L

The DSC and TG curves of GBP powder are shown in Fig. 2A. Obviously, one predominant endothermic peak at 169 °C with enthalpy of 56.47 ± 2.21 kJ/mol may be attributed to the melting of GBP [6,16]. Another two small endothermic peaks at 156 and 207 °C were also observed. The former could be due to a solid-state change, but the latter was attributed to the complete loss of drug. Two steps of weight loss before and after 176 °C were also observed in TG curve. The first-step of weight loss from 160 to 176 °C was about 25.54%, but the second-step of weight loss from 176 to 200 °C was 67.68%. The residual amount was about 6.78%, which was also completely vanished after 260 °C. This weight loss was due to one of the following mechanisms: sublimation, evaporation or decomposition. When preheating the GBP powder to 176 °C and then cooling to 25 °C, the DSC and TG curves of this 176 °C-preheated sample are indicated in Fig. 2B. It is apparent that only an endothermic peak was found at 91 °C with enthalpy of 20.07 ± 0.89 kJ/mol in the DSC thermogram. This temperature was just identical to the melting point of γ -lactam form of GBP [6,16], suggesting the formation of GBP-L via intramolecular cyclization of GBP was occurred after heating GBP sample to 176 °C. Beyond 93 °C, the weight loss was begun and about 98.08% of weight loss was obtained within 93–200 °C. The weight loss was completed after 260 °C. Since the weight loss was beyond the melting point of 91 °C, thus it might possibly relate to the evaporation process, rather than sublimation. At the same time, a thin plate of crystal habit was found in the top place of DSC or TG analytical system. This thin plate crystal form evaporated was proven to be a GBP-L, similar to the report of GBP-L [20]. This implies that the GBP-L was first formed after heating the GBP to 176 °C, and then the GBP-L was evaporated with the increase of temperature. In the process of GBP-L formation, the intramolecular cyclization might be occurred in the GBP structure to liberate one molecule of water, as shown in Scheme 1. However the weight loss in first-step of Fig. 2A was larger than that of the weight loss

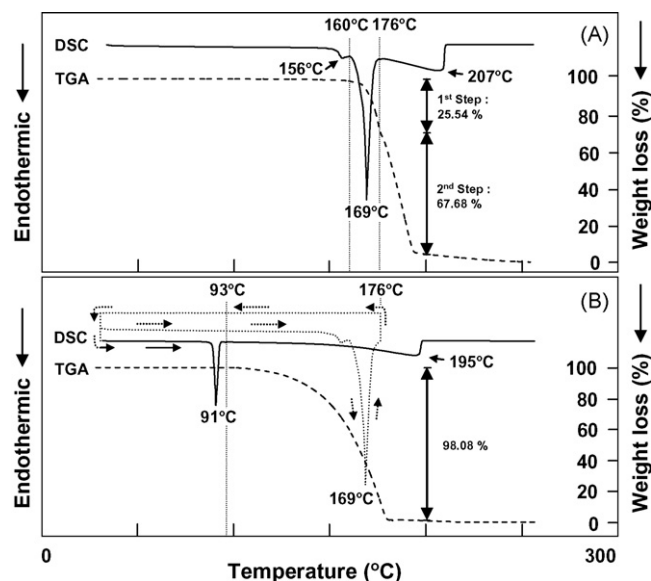
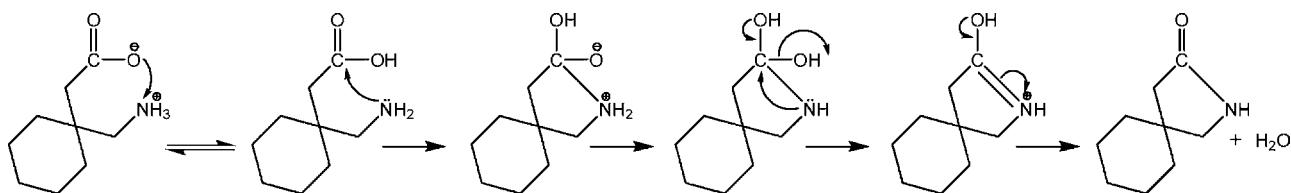


Fig. 2. DSC thermogram and TG curve of GBP (A) and GBP-L (B) powders.



Scheme 1. The proposed pathway for intramolecular lactamization of GBP in the solid state.

of one molecule of water, implying that the evaporation process of water liberated was simultaneously combined to the evaporation process of GBP-L.

Fig. 3 shows the representative FTIR spectra of GBP, GBP-L (176 °C-preheated sample) and the evaporated GBP-L after DSC determination. The raw material of GBP existed as a large rod shaped crystal, but the evaporated GBP-L was found to be a thin plate shaped crystal similar to other report [20]. Since GBP displays a zwitterion in the solid state [13,21], thus there was no IR peak absorption in the usual -NH stretching ($3500\text{--}3300\text{ cm}^{-1}$) but it exhibited an IR band absorption in the region of $3100\text{--}2800\text{ cm}^{-1}$ due to the -NH_3^+ stretching vibration [22]. The peak at 2150 cm^{-1} was corresponded to the distinct side chain and/or CN stretching vibration. In the region of $1700\text{--}1500\text{ cm}^{-1}$, the IR band could be assigned as the ionized asymmetric carboxylate (1615 cm^{-1}) and NH_3^+ deformation vibration (1567 (shoulder) and 1547 cm^{-1}), respectively. From 1500 to 1350 cm^{-1} , these bands corresponded also to the asymmetric carboxylate band and/or CH_2 deformation band. Below 1350 cm^{-1} , these peaks might be used as a fingerprint of GBP. On the other hand, both GBP-L samples exhibited many sharp IR spectral peaks after intramolecular cyclization of GBP. It is evident that several characteristic absorption bands at 3202 (NH stretching), 3098 , 2928 , 2871 (CH stretching), 2845 , 1699 (C=O stretching cyclic), 1678 , 1492 , 1452 (CH bending), 1420 , 1379 , 1330 and 1273 (CN stretching) cm^{-1} were observed in the IR spectra of both GBP-L samples. The IR spectrum of GBP-L formed in this study was markedly consistent with the IR spectrum of GBP-L synthesized at 3204 , 3098 , 2928 , 2870 , 2844 , 1699 , 1675 , 1493 , 1452 , 1420 and 1380 cm^{-1} [23], confirming that GBP-L (176 °C-preheated sample) and the evaporated GBP-L after DSC determination prepared in this study was a pure GBP-L compound.

In order to examine the process of GBP-L formation, different GBP samples were respectively pre-heated to each prescribed temperature by using DSC system, cooled it to $25\text{ }^\circ\text{C}$, and then reheated to $260\text{ }^\circ\text{C}$. The DSC curves of the first- or second-heating GBP samples are shown in Fig. 4. The relationship between the ratio of enthalpy change and temperature is also indicated in Fig. 4. The ratio of enthalpy change in Fig. 4 refers to the ratio of peak enthalpy at $169\text{ }^\circ\text{C}$ for each reheated sample to that of $56.47 \pm 2.21\text{ kJ/mol}$ of intact GBP or at $91\text{ }^\circ\text{C}$ for each reheated sample to that of $20.07 \pm 0.89\text{ kJ/mol}$ of GBP-L evaporated. It clearly shows that before $147\text{ }^\circ\text{C}$ there was no GBP-L formation, and the enthalpy did not change. Once the GBP was preheated to $166\text{ }^\circ\text{C}$ and then reheated, a small peak at $150\text{ }^\circ\text{C}$ was observed. This peak might be presumably due to the sample interaction with the molten GBP-L, which would also influence the enthalpy ratio results. The ratio of enthalpy change was slightly reduced beyond $154\text{ }^\circ\text{C}$ but extensively decreased after $160\text{ }^\circ\text{C}$. At the same time, the formation of GBP-L was markedly obtained by increasing the ratio of enthalpy change of lactam formation due to intramolecular cyclization. At $169\text{ }^\circ\text{C}$, the formation of GBP-L reached to a plateau state and then reduced, due to the evaporation of GBP-L. Since GBP displays a zwitterion in the solid state [13,21], the lactam formation of solid-state GBP might be proposed by the negatively charged carboxyl group in the zwitterion state attacking the protonated amino group of GBP-L, as shown in Scheme 1 [23].

3.2. Process determination by simultaneous DSC–FTIR combined technique

Three-dimensional plots of the FTIR spectra of both GBP and GBP-L samples prepared by 1KBr or 2KBr method as a function

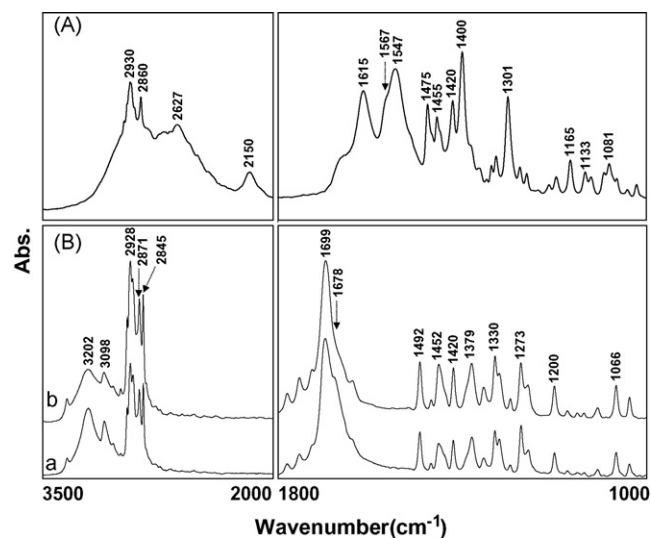


Fig. 3. The representative FTIR spectra of GBP (a), GBP-L (176 °C-preheated sample) (b), and the evaporated GBP-L (c) after DSC determination.

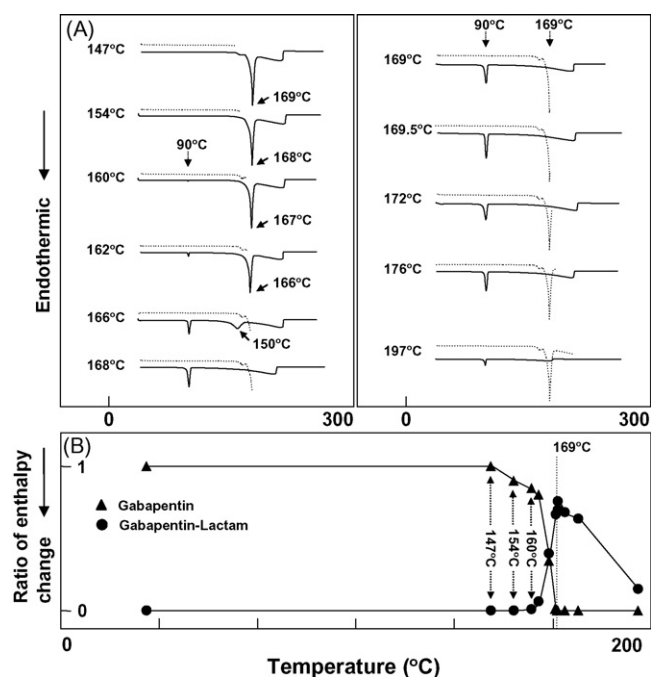


Fig. 4. The DSC thermograms of the first- (dotted line) or second-heating (solid line) GBP samples (A) and the relationship between the ratio of enthalpy change and temperature (B).

of temperature are displayed in Fig. 5. Obviously, the thermal-dependent IR spectral contour of GBP sample prepared by 1KBr method were changed from 147 °C (Fig. 5A). Several broad IR peaks at 3150, 1620, 1533, 1456 and 1374 cm^{-1} were also observed from the IR spectral contour map. These peaks were consistent with that of the IR spectrum of polymorphic form IV of GBP [15], but gradually disappeared with temperature. The IR spectra corresponding to GBP-L formed did not find in this IR spectral contour, due to the quick evaporation of GBP-L from the 1KBr disc once the GBP-L was formed. Three-step process (<147 °C, 141–189 °C, >189 °C) of thermal-related IR spectral changes was obtained for the GBP sample prepared by 1KBr method. Before first-step of 147 °C, there was no any alteration for three-dimensional IR spectral map. In the second-step of 147–184 °C range, changes to the corresponding contour map of these IR spectra were observed. Several specific IR spectral peak intensities were changed markedly. This IR spectral

change was closely related to the corresponding DSC endothermic peak at 169 °C. Here, a slightly increase in peak intensity at 3150 and 1374 cm^{-1} was clearly observed by increasing the temperature, but gradually disappeared from 169 °C. After 184 °C, no sample could be detected due to complete evaporation.

Fig. 5B shows three-dimensional plots of FTIR spectra of GBP sample prepared by 2KBr method as a function of temperature between 4000–2000 and 1800–1000 cm^{-1} . With the increase of temperature, the IR spectral contour and several specific IR frequencies significantly changed. In particular, two new peaks at 1701 and 3350 ($3200\text{--}3400$) cm^{-1} were clearly evidenced. The former was assigned to the carbonyl band of lactam formation of GBP due to intramolecular cyclization; the latter was due to water liberated from sample after intramolecular cyclization. The persistence of the IR spectra of water ranging from 3200 to 3400 cm^{-1} was still observed even at higher temperature, this should be

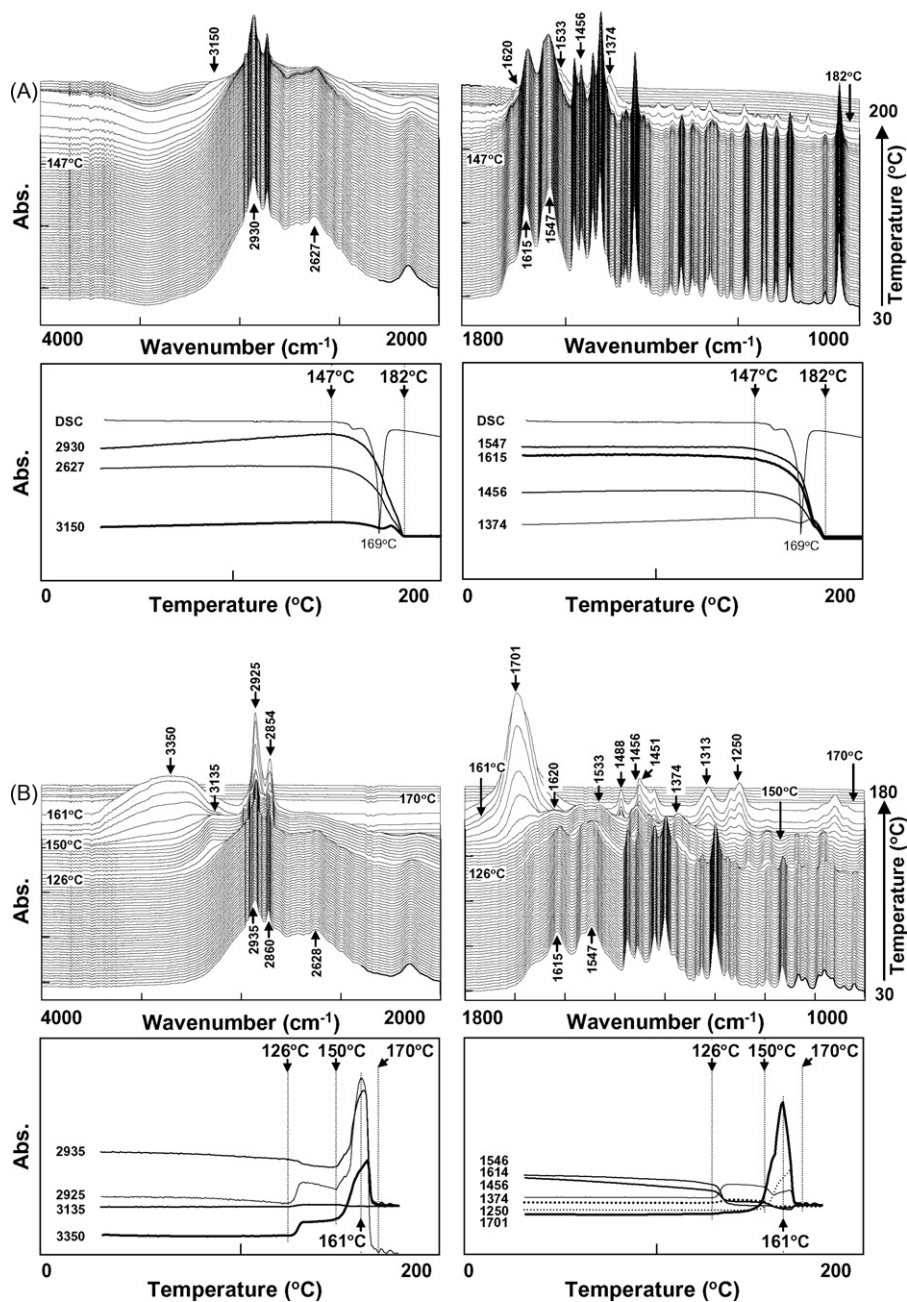


Fig. 5. Three-dimensional plots of the FTIR spectra of both GBP and GBP-L samples prepared by 1KBr or 2KBr method as a function of temperature. Key: (A) GBP sample prepared by 1KBr method. (B) GBP sample prepared by 2KBr method. (C) GBP-L sample prepared by 1KBr method.

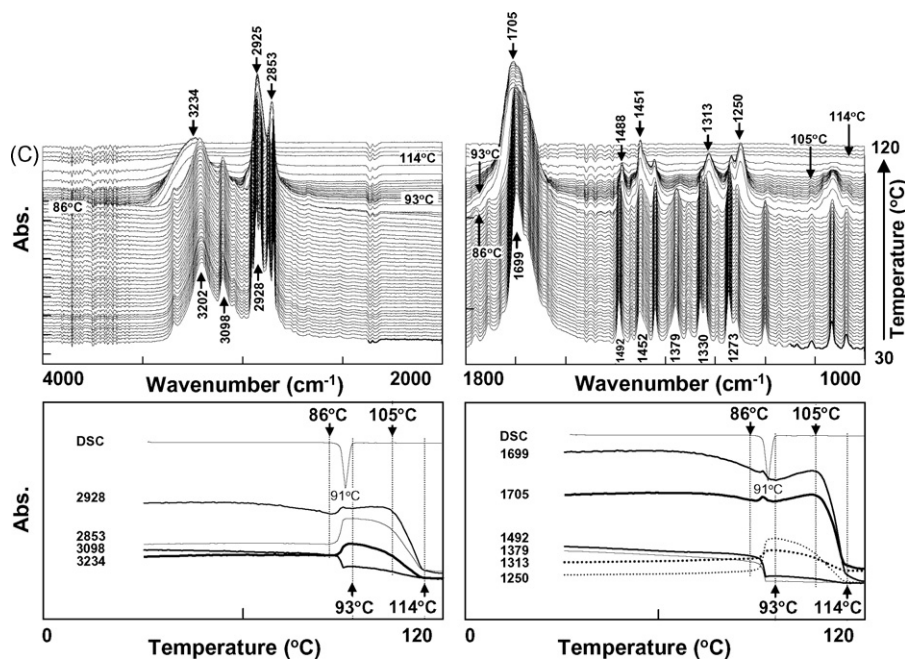


Fig. 5. (Continued).

attributed to the by-product “water” being tightly sealed within 2KBr pellets. The interaction of water with KBr might shift the peak from 3500 cm^{-1} (assigned to free water) to a lower wavenumber ($3200\text{--}3400\text{ cm}^{-1}$). By increasing the temperature, however, these predominant peaks at 1701 and 3350 cm^{-1} also disappeared, due to the evaporation of water and GBP-L. Five-step process ($<126^\circ\text{C}$, $126\text{--}150^\circ\text{C}$, $150\text{--}161^\circ\text{C}$, $161\text{--}170^\circ\text{C}$, $>170^\circ\text{C}$) of thermal-dependent IR spectral changes of GBP sample prepared by 2KBr method was also detected. Before first-step of 126°C , there was no change in IR spectra. A second-step was formed within $126\text{--}150^\circ\text{C}$, the IR spectra was similar to that of the IR spectra of second-step of GBP prepared by 1KBr method, in which the peaks at 3150 , 1620 , 1533 , 1456 and 1374 cm^{-1} were observed due to the polymorphic form IV formation of GBP [15]. Another investigation of the polymorphic formation and transformation of GBP is currently being carried out [24]. Further heating ($150\text{--}161^\circ\text{C}$), several new IR peaks at 3350 , 1701 , 1488 , 1451 , 1313 and 1250 cm^{-1} were found. These peaks except 3350 cm^{-1} are similar to that of the IR spectra of GBP-L after heating to 93°C (Fig. 5C). This step was corresponded to the lactam formation of GBP, in which the peak at 3350 cm^{-1} assigned to water was evidenced. In the temperature of $161\text{--}170^\circ\text{C}$, the GBP-L was markedly evaporated from the cranned KBr disc, leading to the quick reduction of IR spectral peak intensity. After 170°C , no sample could be detected due to complete evaporation. Since the GBP was sealed within 2KBr pellets, the evaporation of GBP-L formed was delayed by the tight compact, leading to the temporary observation from the three-dimensional IR spectral plot of GBP-L. This suggests that the process of intramolecular lactamization GBP was easily determined in the GBP sample prepared by 2KBr method rather than 1KBr method.

Three-dimensional plots of FTIR spectra of GBP-L sample prepared by 1KBr method as a function of temperature between $4000\text{--}2000$ and $1800\text{--}1000\text{ cm}^{-1}$ is also shown in Fig. 5C. Four-step ($<86^\circ\text{C}$, $86\text{--}93^\circ\text{C}$, $93\text{--}114^\circ\text{C}$, $>114^\circ\text{C}$) of the thermal-dependent IR spectral changes of GBP-L was observed. Several specific IR spectral peaks at 3202 , 1699 , 1492 , 1330 and 1273 cm^{-1} were respectively shifted to 3234 , 1705 , 1488 , 1313 and 1250 cm^{-1} when GBP-L was heated over 86°C , this shifting phenomena was due to the thermal effect and/or chemical/phase changes on the structure of GBP-

L. Moreover, the peaks at 1699 and 3202 cm^{-1} blue-shifted with increasing temperature might be due to that the hydrogen bonds had become weaker and longer [25,26]. Beyond 93°C , these peak intensities were gradually reduced with temperature. After 114°C , the sample was almost completely evaporated.

3.3. Non-isothermal kinetic analysis studied by TG analysis

TG analysis is an optimal method to determine the thermal stability parameters such as dehydration, sublimation, evaporation and decomposition by the kinetics of weight loss from samples. Evaporation is defined as the transition from the liquid phase to the vapor phase and it can be monitored by determining the weight loss as the substance goes through the transition. From the result of Fig. 5B, the processes for water loss from intramolecular lactamization of GBP and evaporation of GBP-L were combined together [14], the combined kinetics of both processes will be examined by a non-isothermal kinetic analysis. According to non-isothermal kinetic models, TG analysis was performed by six heating rates at 2 , 3 , 5 , 8 , 10 and $15^\circ\text{C}/\text{min}$. TG curves were shifted to higher temperatures with increasing heating rates (Figs. 6 and 7). Therefore, Ozawa–Flynn–Wall equation (Eq. (1)) was applied to describe the overall reactions of intramolecular cyclization of GBP and evaporation of GBP-L [27–30]. The data generated could be analyzed and manipulated by model-free approach to obtain the Arrhenius kinetic parameter of activation energy (E_a). Thus, the E_a of non-isothermally intramolecular lactamization of GBP and evaporation of GBP-L was calculated as follows:

$$E_a = \frac{R}{b} \left[\frac{d \log \beta}{d(1/T)} \right] \quad (1)$$

where β is the heating rate ($^\circ\text{C}/\text{min}$), R the gas constant ($8.314\text{ J}/(\text{mol K})$), T the absolute temperature (K), b the constant (0.457) and E_a is the apparent activation energy (J/mol).

By plotting the logarithm of the heating rate vs. the reciprocal of temperature at constant conversion (α), the slope of $0.457E_a/R$ for straight line of this plot was obtained. The apparent E_a was calculated from the slope at different extent of conversion (in the range

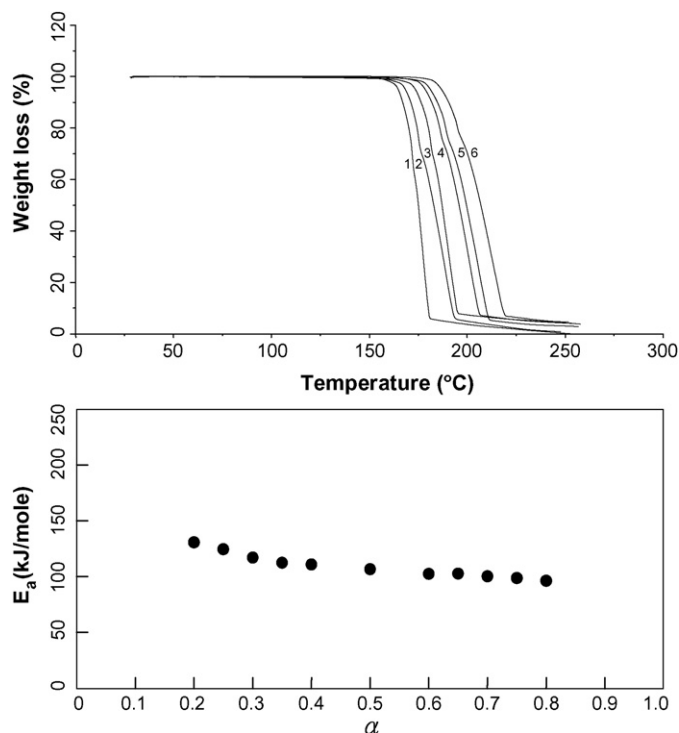


Fig. 6. TG curves of GBP at different heating rates (upper) and dependence of the activation energy vs. degree of conversion for GBP (lower). Key: different heating rates ($^{\circ}\text{C}/\text{min}$): (1) 2; (2) 3; (3) 5; (4) 8; (5) 10; (6) 15.

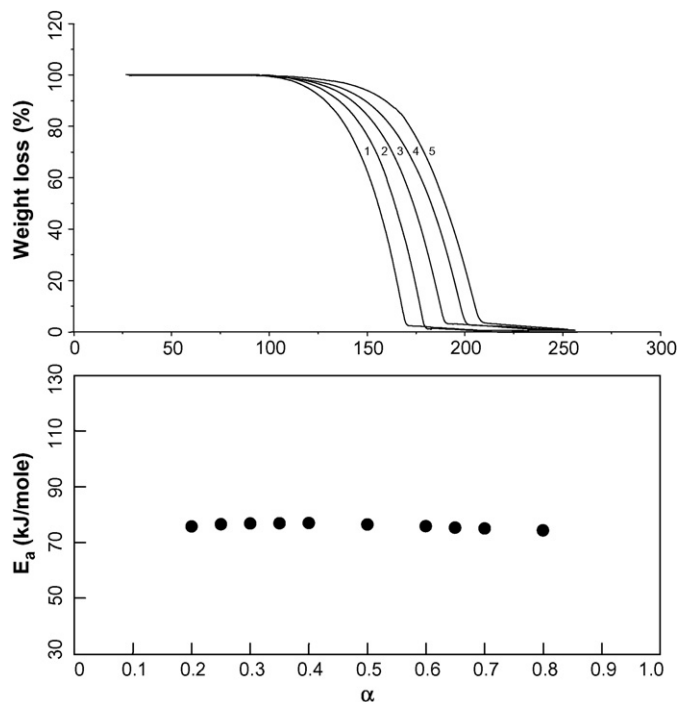


Fig. 7. TG curves of GBP-L at different heating rates (upper) and dependence of the activation energy vs. degree of conversion for GBP-L (lower). Key: different heating rates ($^{\circ}\text{C}/\text{min}$): (1) 2; (2) 3; (3) 5; (4) 8; (5) 10.

of $0.2 \sim \alpha \sim 0.8$) using Eq. (1). All the correlation coefficients were larger than 0.9987. Fig. 6 also shows the dependence of the apparent E_a as a function of conversion, its mean value for the combined reactions of intramolecular cyclization of GBP and evaporation of GBP-L was 114.3 ± 23.3 kJ/mol. Fig. 7 displays the dependence of the

apparent E_a as a function of conversion for the evaporation kinetic of GBP-L too. The apparent E_a value for the evaporation of GBP-L alone was 76.2 ± 1.5 kJ/mol in the range of $0.2 \sim \alpha \sim 0.8$. The relatively uniform E_a values suggests the evaporation of GBP-L was independent of α , but was clearly different from that of the combined reactions of both intramolecular cyclization of GBP and evaporation of GBP-L.

4. Conclusions

The thermodynamics and activation energy of GBP in the solid state were non-isothermally evaluated by DSC and TG techniques. This study clearly indicates that the combined processes of intramolecular lactamization of GBP and evaporation of GBP-L were continuously occurred after melting of GBP, in which the apparent E_a of the combined process was about 114.3 ± 23.3 kJ/mol but the apparent E_a of evaporation of GBP-L alone was 76.2 ± 1.5 kJ/mol. This combined process could not be separated even with a slower heating rate. A powerful simultaneous DSC–FTIR combined technique was easily used to investigate the detailed kinetic processes of intramolecular cyclization of GPBT and evaporation of GBP-L in the solid state.

Acknowledgement

We would like to acknowledge Orient Europharma Co., Ltd. (Taoyuan, Taiwan, ROC) for the kind gift of pharmaceutical grade of gabapentin.

References

- [1] M.J. McLean, B.E. Gidal, *Clin. Ther.* 25 (2003) 1382–1406.
- [2] J.K. Baillie, I. Power, *Curr. Opin. Invest. Drugs* 7 (2006) 33–39.
- [3] G. Chouinard, J. Psychiatry Neurosci. 31 (2006) 168–176.
- [4] G.J. Sills, *Curr. Opin. Pharmacol.* 6 (2006) 108–113.
- [5] L.D. Errante, A. Williamson, D.D. Spencer, O.A. Petroff, *Epilepsy Res.* 49 (2002) 203–210.
- [6] B. Ciavarella, A. Gupta, V.A. Sayeed, M.A. Khan, P.J. Faustino, *J. Pharm. Biomed. Anal.* 43 (2007) 1647–1653.
- [7] H. Potschka, T.J. Feuerstein, W. Loscher, *Naunyn Schmiedebergs Arch. Pharmacol.* 361 (2000) 200–205.
- [8] W.A. Lagrèze, R. Muller-Velten, T.J. Feuerstein, *Graefes Arch. Clin. Exp. Ophthalmol.* 239 (2001) 845–849.
- [9] F. Henle, J. Leemhuis, C. Fischer, H.H. Bock, K. Lindemeyer, T.J. Feuerstein, D.K. Meyer, *J. Pharmacol. Exp. Ther.* 319 (2006) 181–191.
- [10] S.R. Byrn, R.R. Pfeiffer, J.G. Stowell (Eds.), *Solid-state Chemistry of Drugs*, 2nd ed., SSCI, Inc., West Lafayette, Indiana, USA, 1999.
- [11] S.R. Byrn, W. Xu, A.W. Newman, *Adv. Drug Deliv. Rev.* 48 (2001) 115–136.
- [12] A. Khawam, D.R. Flanagan, *J. Pharm. Sci.* 95 (2006) 472–498.
- [13] H.A. Reece, D.C. Levendis, *Acta Crystallogr. C* 64 (2008) 105–108.
- [14] D. Braga, F. Grepioni, L. Maini, K. Rubini, M. Polito, R. Brescello, L. Cotarca, M.T. Duarte, V. André, M.F.M. Piedade, *New J. Chem.* 32 (2008) 1788–1795.
- [15] S. Chava, R.G. Seeta, K.I.V. Sunil, WO2004110342 (2004).
- [16] A. Cutrignelli, N. Denora, A. Lopodota, A. Trapani, V. Laquintana, A. Latrofa, G. Trapani, G. Liso, *Int. J. Pharm.* 332 (2007) 98–106.
- [17] M. Pesachovich, G. Singer, G. Pilarski, US 6,255,526 (2001).
- [18] S.Y. Lin, J.L. Chien, *Pharm. Res.* 20 (2003) 1926–1931.
- [19] S.L. Wang, S.Y. Lin, T.F. Hsieh, S.A. Chan, *J. Pharm. Biomed. Anal.* 43 (2007) 457–463.
- [20] K. Ananda, S. Aravinda, P.G. Vasudev, K.M. Poopathi Raja, H. Sivaramkrishnan, K. Nagarajan, N. Shamala, P. Balaram, *Curr. Sci.* 85 (2003) 1002–1011.
- [21] J.A. Ibers, *Acta Crystallogr. C* 57 (2001) 641–643.
- [22] S.A. Chimatadara, T. Basavaraja, K.A. Thabaja, T. Sharanappa, *J. Mol. Catal. A: Chem.* 267 (2007) 65–71.
- [23] S. Roller, C. Siegers, R. Haag, *Tetrahedron* 60 (2004) 8711–8720.
- [24] C.H. Hsu, S.Y. Lin., unpublished results, 2008.
- [25] D. Hadzi, S. Bratos, *Vibrational spectroscopy of the hydrogen bond*, in: P. Schuster, G. Zundel, C. Sandorfy (Eds.), *The Hydrogen Bond*, vol. II, Elsevier, Amsterdam, 1976 (chapter 12).
- [26] A. Novak, *Struct. Bond.* 18 (1974) 177–216.
- [27] T. Ozawa, *Bull. Chem. Soc. Jpn.* 38 (1965) 1881–1886.
- [28] J.H. Flynn, L.A. Wall, *J. Polym. Sci. Polym. Lett.* 4 (1966) 323–328.
- [29] S.Y. Tsai, S.C. Kuo, S.Y. Lin, *J. Pharm. Sci.* 82 (1993) 1250–1254.
- [30] F. Rodante, S. Vecchio, G. Favero, *J. Therm. Anal. Calori.* 74 (2003) 121–139.